Turkish Journal of Electrical Engineering & Computer Sciences

http://journals.tubitak.gov.tr/elektrik/

Research Article

Turk J Elec Eng & Comp Sci
(2022) 30: 818 – 838
© TÜBİTAK
doi:10.3906/elk-2106-2

Reactive power sharing and voltage restoration in islanded AC microgrids

Khurram Hashmi[1,*], Rizwan Ali[1], Muhammad Hanan[2], Waseem Aslam[3], Abubakar Siddique[4], Muhammad Mansoor Khan[5]

[1]Department of Electrical Engineering, University of Engineering and Technology, Lahore
[2]State Key Laboratory of Alternate Electrical Power System with Renewable Energy Sources, School of Electrical and Electronic Engineering, North China Electric Power University, Beijing, China
[3]Department of Electrical Engineering University of Sargodha, Punjab, Pakistan
[4]Department of Electrical Engineering, Khwaja Fareed University of Engineering and Information Technology (KFUEIT), Rahim Yar Khan, Pakistan
[5]School of Electronics Information and Electrical Engineering (SEIEE), Shanghai Jiao tong University, Shanghai, China,

Received: 01.06.2021 • **Accepted/Published Online:** 28.10.2021 • **Final Version:** 21.03.2022

Abstract: Microgrids (MG) are a new and innovative concept in modern distribution networks. Several challenges are associated with the operation and control of MG networks. Active and reactive power sharing among energy resources interfaced through power electronic conversion stages is a major challenge. Although active power sharing can be achieved under varying scenarios, sharing of reactive power between distributed generation units is difficult to achieve. This paper presents a novel and innovative control scheme to ensure sharing of reactive power between Distributed generation units within an autonomous, islanded AC microgrid. A framework composed of novel multiagent moving average estimators is proposed to make the participating nodes share active and reactive power among themselves. Detailed case studies are carried out in MATLAB and Simulink environment to verify the efficacy of the proposed control scheme. Furthermore, a lab scale MG set up is implemented to verify the operation of the control scheme in an MG environment.

Key words: Reactive power sharing, microgrids, power electronics, voltage regulation, frequency regulation

1. Introduction

Active and reactive power regulation is a major area of investigation in microgrid control. If we consider steady state conditions for a microgrid operation where all DGUs operate at the same nominal frequency, active power can be effectively monitored using enhanced droop control designs. However, it has been observed that reactive power sharing remains insufficient and harmonic power appears in DGU power conversion stages during unequal feeder impedances and nonlinear load conditions. Circulating reactive powers among DGUs and system instability may be attributed to insufficient reactive power sharing [1] The P-V and Q-f droop scheme is viable for smaller networks where the nature of the network is largely resistive. For larger networks the nature of the network impedance becomes inductive and a P-f and Q-V relationship for droop coefficients is more favorable [2]. For better performance a virtual impedance control is combined with the conventional droop method, that makes the network virtually more inductive and improves the control performance [3, 4].

The action of the reactive and active power sharing droop causes the voltage and frequency regulation to deteriorate, respectively. A secondary monitoring and corrective control layer is required to decrease the

*Correspondence: Correspondence: khurramhashmi@uet.edu.pk

error among the nominal and actual bus voltages. The corrective terms are made to go through PI controller to minimize the errors. However, the conventional PI based secondary controller has opposite effect to the primary reactive power sharing controls. Therefore, the reactive power sharing between nodes deteriorates as a result of the secondary corrective controls [5, 6]. Furthermore, the conventional reactive power sharing methods are ineffective for mismatched feeder impedances and incomplex network structures. Several strategies have been studied in the literature to address this issue. Some decentralized strategies combine adaptive droop strategies with virtual impedance method to enhance control performance [7]. Several combinations of virtual impedance method and consensus-based control are presented.

Frequency, voltage stability, active and reactive power sharing are all essential requirements for the smooth operation of the MG. Conventional hierarchical control procedures must be enhanced to regulate these parameters for MG systems effectively [8, 9].

The most popular methods to solve voltage regulation along with reactive power sharing can be divided into three sections: optimizing the secondary control equations, using programming algorithms to give scheduled power references, and multiagent system based algorithms [10, 11]. Distributed average proportional-integral (DAPI) methods consisting of graph theory are shown in [12] for reactive power sharing. However, realizing voltage regulation or reactive power sharing cannot be addressed simultaneously despite the tuning of DAPI controllers [13].

Consensus-based distributed control methods [14] are used to obtain proportional power sharing by combining the droop and secondary control into one and coordinating the controllers over a sparsely connected network. Voltage references are generated by excluding reactive power and amplitude mismatch by PI controllers and consensus observers. A multiagent based control system can be used to control reactive power in an islanded grid. The MAS forms a group of agents where each agent has some degree of intelligence and exercises a certain degree of autonomy to make its decisions.

Various droop-based techniques have been suggested in the literature to share reactive power among nodes. These can be defined into three major categories: the improved primary droop methods, the improved virtual impedance methods, and the improved hierarchical control methods.

Some approaches utilize an adaptive voltage droop control to distribute the reactive power [15]. The adaptive droop coefficients compensate the mismatched feeder impedances' effect for distributing reactive power. In order to trace unbalanced and reactive powers, an efficient inverse control with the enhanced droop control algorithm is recommended to set the weight coefficients of filters in real time. Though, the reactive power sharing of islanded MG is inadequate during unbalanced and nonlinear load situations.

To achieve a better sharing of reactive power between different DGUs in an island MG, the control method for reactive power sharing should be significantly enhanced. Also, more resilience needs to be added to the control scheme to resist communication latencies and failures. The suggested method improves the convergence speed and accuracy of reactive power sharing between DGUs. Improved distributed value estimation observers proposed in this paper are used to provide accurate average estimated to ensure convergence of system values within short time span.

2. A background of reactive power sharing in MGs

Reactive power sharing is required in distribution networks to balance voltage sags and swells. Traditionally reactive power sharing has been delegated to dedicated power electronics devices as SVC and static switched capacitors. However, in power electronics based microgrids, the reactive power management goals may be achieved through distributed power electronic converters. Several control modifications are made to ensure a sharing of reactive power between distributed power generation units throughout the microgrid network.

It remains a challenge to share reactive power within mismatched feeder impedances effectively. Nonlinear and unbalanced load conditions add further problems to the power sharing problem. The techniques based on virtual impedance or enhanced virtual impedance was suggested as an alternative to the enhanced droop controls to distribute the active and reactive powers. Although the inductive virtual impedance during the mismatched feeder impedance situation can enhance the reactive power sharing capability, the reactive power cannot be distributed precisely when the loads in islanded MGs are nonlinear and unbalance.

A hierarchical control-based self-adjusting approach is established to distribute the reactive power through the adaptive droop control and recover the voltage amplitude and frequency through the secondary control to the rating value [16]. Furthermore, the control scheme for the distribution of reactive power is defined in [17], which consolidates the MGCC (microgrid central controller) and the droop control. The MGCC is used to determine the average reactive power and change comparisons to similar DG units for reactive power. The MG's physical modes are complicated, and the delay in communication can severely affect the reactive capacity.

The control and power control for islanded MGs is presented in most of the existing works. At the same time, the difficulties of power sharing with incompatible feeder impedance and nonlinear loads are rarely totally taken into account [18]. The voltage reference is created in [19] using the positive-sequence power. In the meantime, for the unbalanced voltage correction to differentiate load power sharing, the negative-sequence reaction control is used. In [20], the technique developed for power sharing is proposed to extend the reactive power of the islanded MG everywhere it decreases in frequency, to reduce reactive, balanced and harmonic problems in power sharing. The undefined feeder impedances can be compensated by the virtual impedance of the MG variable and the frequency droop control interactions. Absolute reactive power sharing in a constant state is made. The lack of the impedance and nonlinear and unbalanced loads of the DG feeder generated by MGs through additional GM research and touch delay in the low bandwidth communication lines (LBC) show that there remains need of further research for improvement in the control approaches for the actual sharing of reactive power. The programming algorithm is provided in [21] to ensure that the system is safe and that reactive power sharing is correct. In [22] introduces the approach to stochastic reactive power management which uses spontaneous active injections of power to accomplish an online reactive power control approach. This method is entirely distributed and involves active power injection only. Realizing that the unmanageable RES is vulnerable to the external environment, an agent-based approach to stabilizing the active and reactive powers is implemented [23]. Because the communication delay frequently presents in hierarchical monitoring, the higher level command signals are transmitted to primary controls encounter a time lag due to the communication lines, creating harm to microgrid systems. We must acknowledge the communication delay generated by the LBC lines to obtain better active and reactive power sharing. The method of a gain scheduler in [24] is used to correct the secondary control reference signal and mitigate the effect of the LBC delay. In [25], the use of the predictive control design is often used to reduce this effect. In order to explain reactive power sharing by recognizing the delay of contact for MG, a cooperatively distributed secondary/primary control criterion is also applied [26]. The droop coefficient is theoretically adopted if the feeder impedance is nearly inductive (resistance is insignificant). The active power can be distributed, but some deficiencies in the traditional droop control for reactive power sharing are unavoidable.

The droop coefficient must be negligible for the short-range of frequency variations, which violates distributing active power. A higher droop coefficient, however, would increase the output of active power sharing, this results in a greater divergence of voltage from nominal values [27, 28]. In the traditional droop control, only equal active power sharing can be ensured under the inductive feeder impedance case. Furthermore, the precision of active power sharing can be undermined, and active and reactive power connection can arise in resistive systems. It is also unlikely to achieve an active proportional power sharing [29]. Since there may be different DG types, the traditional droop control cannot decrease the cost of generation for the MG considered.

Series-cascaded microgrids are investigated that are formed by dispatchable and nondispatchable DGUs. A decentralized master slave control scheme that regulates voltage and frequency and maintains power balance. The proposed method promises maximum utilization of nondispatchable power resources, autonomous power curtailment under light load, increase system reliability [30]. A distributed event-triggered power sharing control strategy is proposed in this paper. The suggested technique adaptively regulates the virtual impedances at both fundamental positive/negative sequence and harmonic frequencies and, therefore, accurately share the reactive, unbalanced, and harmonics powers among distributed generation (DG) units. The proposed method requires no information of feeder impedance and involves exchanging information among units at only event triggered times, which reduces the communication burden without affecting the system performance. The stability and interevent interval are analyzed in this paper [31].

A generalized proportional-integral finite-time controller (GPI-FTC) is proposed. The GPI-FTC is synthesized based on the control Lyapunov function method and modifying the conventional PI controller by adding a consensus term to the integrand dynamic. The proposed distributed GPI-FTC provides plug and play capability, scalability, and fast finite-time convergence of the system states. Moreover, a reactive power sharing (Q-sharing) method is designed to improve the sharing pattern of reactive power under exact voltage regulation. Also, a distributed voltage observer is developed for average voltage regulation [32].

A distributed reactive power sharing control problem for an autonomous inverter-based microgrid with resilience for communication faults, which may be caused by partial communication link failures or some channel manipulation attacks. Under the standard decoupling approximation for bus angle differences, the reactive power flow of each inverter can be controlled by manipulating the voltage amplitudes of itself and its neighbour inverters. By designing an adaptive resilient cooperative control scheme, accurate reactive power sharing can be guaranteed even in the presence of communication faults [33]. Therefore, controllers at higher levels often have to be redesigned whenever a different power grid is considered, hence, incurring higher cost and effort. As a way to overcome that problem, in this work, a unified secondary controller using distributed control theory is designed for different droop schemes associated with distributed battery storage in different grid conditions. The control design follows the consensus theory, originally designed for multiagent systems, to control the frequency and voltage at the point of common coupling (PCC), synchronize energy levels, and proportionally share active and reactive powers of battery storage systems. A sufficient condition for the upper bound of communication delays between storage systems is derived to ensure system stability. Several scenarios are studied using a modified IEEE 118-bus benchmark to support the theoretical results of the proposed approach [34].

A new two level control scheme is proposed for accurate power sharing and appropriate voltage regulation in dc MGs during islanded operation mode. In the primary control level, a P-V droop method is proposed to eliminate the dependency of power sharing among DERs on line resistances. Since the P-V droop deviates the voltage derivative to a nonzero value, a voltage derivative restoration mechanism is adopted in the secondary control level to provide voltage stability. The secondary control level also compensates the voltage deviations by cascading an outer voltage control loop with the inner voltage derivative restoration loop. The secondary control signal is broadcasted to each DER via a unidirectional low-bandwidth communication link [35].

In short, to achieve a better sharing of reactive power between different DGUs in an island MG, the control method for reactive power sharing should be significantly enhanced. Also, more resilience needs to be added to the control scheme to resist communication latencies and failures. The suggested method improves the convergence speed and accuracy of reactive power sharing between DGUs. Improved distributed value estimation observers proposed in this paper are used to provide accurate average estimated to ensure convergence of system values within short time span

Most of the reactive power sharing mechanisms fail to substantially share reactive power in islanded microgrids. Reactive power sharing is often achieved at the expense of voltage restoration. This work proposes a novel control method to share reactive power and also restore voltage levels.

3. Proposed distributed average estimators

A novel active and reactive power sharing control is suggested herein. Key benefits of multiagent system MAS are balance power and energy, stabilizing voltage and frequency, and economic coordinated operation between microgrids and microgrid clusters. Designing of MAS are based on different types of mathematical models like graph topology models, noncooperative game model, genetic algorithm, and particle swarm optimization algorithm. Operation of MAS depends upon communication links, delay in these links leads to stability issues. These delays vary from 10's to several hundred milliseconds. Thera are two types of delays, fixed and random communication delay. Schemes used to compensate the fixed type of delays are neural network predictive control (NPC), weighted average predictive control, gain scheduling, and synchronization schemes using multi-timer model. And schemes that used to fix random delay are generalized predictive control (GPC), model predictive control (MPC), Smith predictor (SP), H control, and sliding mode control.

Today distributed energy resources being used all over the world effectively. Operation of distributed energy resources can be governed by power grid or can be operated in autonomous mode. Operation in governed system in quite easier but when operate in autonomous mode droop control required.

In decentralized system power-frequency and reactive power-voltage droop controls are used. With P-f droop control an accurate active power sharing achieved among distributed energy resources. But in reactive power sharing the Q-V droop control totally depended upon filter and power line impedance. The line impedance varies with the changing of distance and the filler impedance depends on design and system properties. So, by varying these impedances the total impedance changes there for the Q-V droop control effected. Proposed scheme to overcome this problem is voltages restoration, in which the reactive power sharing independent form line impedance. In proposed scheme output voltages are resulted by integrating voltages and keep varying the voltage until the required reactive sharing achieved. By controlling the droop coefficient nx and restoration gain Kres the reactive power sharing can be easily controlled.

This strategy relies on a regulated ”droop” concept that draws on the concept of finite impulse response filters (FIR) and infinite impulse response filter (IIR) [36]. Each node shall be configured with the distributed medium power observers/estimators, as presented in Figures 1. Active and reactive power controller is shown in Figure 1a, true average power observers and quasi-average observers are presented in Figures 1b and 1c, respectively. An analysis obtained from adjacent nodes and local measurements indicates that both system nodes attain average amounts of injected power. Equations 1 and 2 show that the mean power is employed for local droop-based controls as a reference. To achieve distribution of active and reactive power equations the frequency and voltage are proportionally modified in order to mathematically represent the proposed power controller.

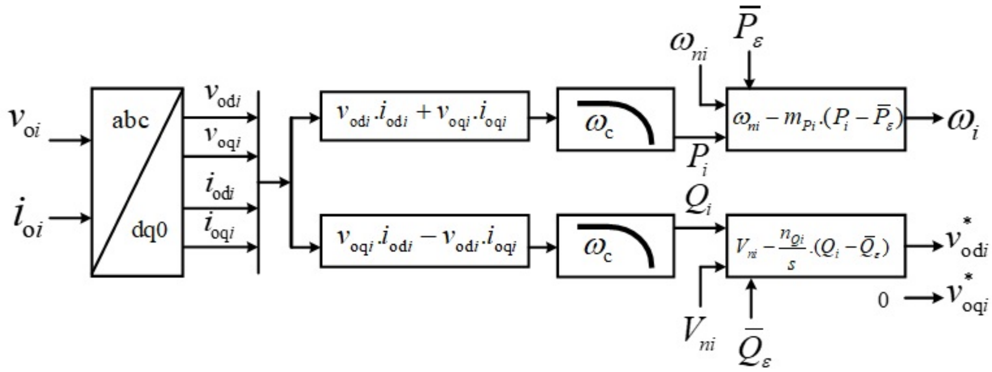

(a) Active and reactive power controllers.

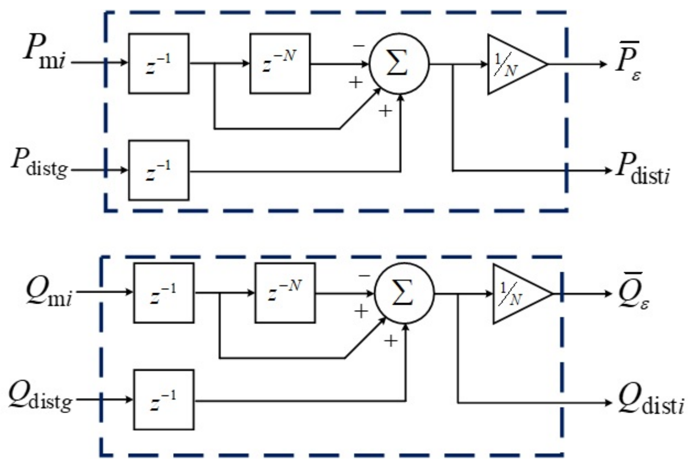

(b) True average power observers.

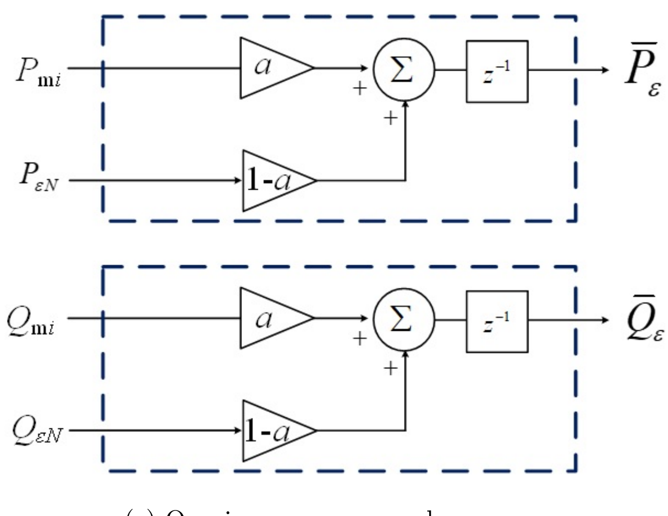

(c) Quasi-average power observers.

Figure 1. Power controllers.

$$\omega_i^* = \omega_{ri} - m_{Pi}(P_i - \overline{P}_\varepsilon) \quad (1)$$

$$\begin{cases} v_{odi}^* = V_{ni} + \frac{N_{Qi}(Q_i - \overline{Q_\varepsilon})}{s} \\ V_{oqi}^* = 0 \\ V_o = \sqrt{(v_{odi}^*)^2 + (v_{oqi}^*)^2} \end{cases} \quad (2)$$

$$X_m = [P_m, Q_m, \omega_m, v_m] \quad (3)$$

$$X_{avg\ i}(k+1) = \frac{X_{m,i}(k-1) - X_{m,i}(k-(N+1)) + X_{d,inst,g}(k-1)}{N} \quad (4)$$

$$\begin{cases} \Delta X_{m,i} = X_{m,i}(k-1) - X_{m,i}(k-(N+1)) \\ X_{d,ist,i} = \Delta X_{m,i} + X_{dist,g}(k-1) \\ V_{avg,i}(k+1) = \frac{\Delta X_{m,i} + X_dist,g(k-1)}{N} \\ X_e = X_{m,i} + X_{avg,i} \end{cases} \quad (5)$$

$$\overline{X}_{\varepsilon i} = [\overline{P}_{\varepsilon i}, \overline{Q}_{\varepsilon i}, \overline{\omega}_{\varepsilon i}, \overline{v}_{\varepsilon i}] \quad (6)$$

In equations, the number of nodes is denoted by N, the present node is denoted by I, the averaged power transferred among nodes is denoted by X_{avg} the average obtained from the neighbor node is denoted by $X_{dist,g}$ and the average values computed is denoted by $X_{dist,i}$ and sent out by node $i.X_{mi}$ is the vector of values measured at each node. $x_{\varepsilon,i}$ represent a vector of averaged estimations calculated at the node. $\overline{P}_{\varepsilon,i}$ represents estimated active power; $\overline{Q}_{\varepsilon,i}$ represents reactive power, $\overline{\omega}_{\varepsilon,i}$ represents estimated frequency; $\overline{v}_{\varepsilon,i}$ represents estimated voltage. Likewise, $P_{m,i}$ represents measured active power; $Q_{m,i}$ represents measured reactive power, $\omega_{m,i}$ represents measured frequency; $v_{m,i}$ represents measured voltage. v_{odi}^* and v_{oqi}^* represent the references for voltage controller.

4. Secondary layer controls: voltage and frequency regulation

The suggested voltage and frequency regulation method is implemented through a novel distributed averaging based secondary controls [37]. The distributed frequency and voltage control design is shown in Figure 2.

The frequency regulation formula has been formed by

$$\begin{cases} \omega_{ni}(k+1) = \omega_{\mathrm{oi}}(k) + k_{\mathrm{pf}} e_{\omega i}(k) + k_{\mathrm{if}} \sum_{i=ko}^{k} e_{\omega i}(k) \\ e_{\omega i}(k+1) = (\bar{\omega}_\varepsilon(k) - \omega_{\mathrm{oi}}(k)) + (\omega_{\mathrm{ref}}(k) - \omega_{\mathrm{oi}}(k)) \end{cases} \quad (7)$$

The nominal frequency of reference is provided by ω_{ref} , the calculated frequency of system is presented as ω_{oi} that is calculated at the local node; ω gives the averaged frequency calculated by the suggested observers. k_{pf} and kif shown in Figure 2 are the secondary frequency restores relative and integral gains. ω_{ni} describes the updated frequency relation of the i-th inverter.
The voltage regulation method is described as:

$$\begin{cases} V_{ni}(k+1) = v_{oi}(k) + k_{pv} e_{vi}(k) + k_v \sum_{i=ko}^{k} e_{vi}(k) \\ e_{vi}(k+1) = (\overline{v}_\varepsilon(k) - v_{oi}(k)) + (v_{ref}(k) - v_{oi}(k)) \end{cases} \quad (8)$$

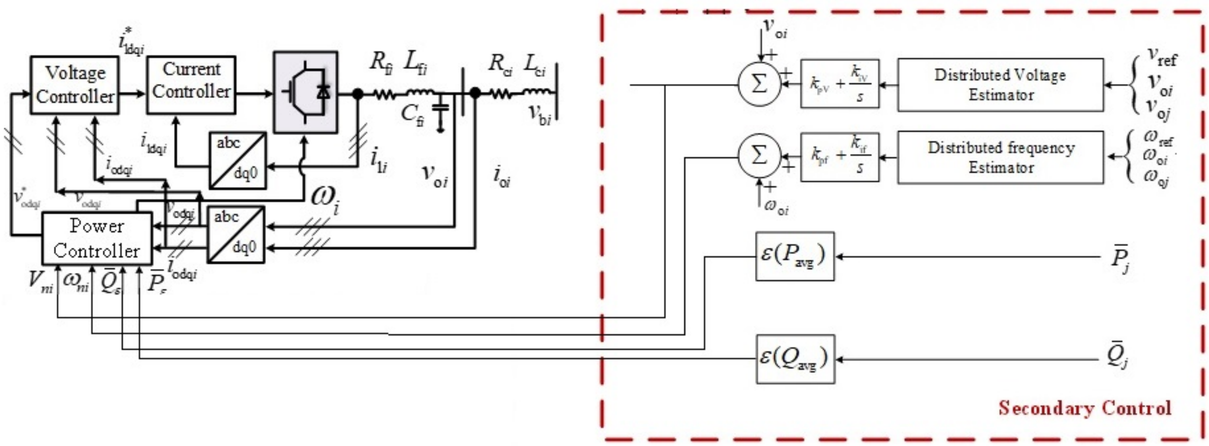

Figure 2. Distributed control scheme: secondary controls at every node.

where system's nominal reference voltage is represented by v_{ref} and v_{oi} is the system voltage calculated local node i being considered v_{ε}. This gives the averaged voltage calculated by the suggested observers. For the secondary voltage restoration, the proportional and integral gains are described as k_{pv} and k_{iv} as represented in Figure 2. V_{ni} is the updated reference of voltage for the i-th inverter node.

5. A comparison of estimators

The suggested system would converge in negligibly less time for a limited number of nodes as compared to consensus-based controls. It can be suggested in this case that the suggested FIR-based technique is more effective.

In comparison, quasi averaging estimators, inspired from infinite impulse response filters (IIR), function differently. Although these are based on the same principle as distributed averaging, they strive to arrive at a "quasi" average or a near-average of the system value. The suggested estimator constructs the output in relation to an infinite number of samples [36]. When the time delay td increases, IIR convergence slows down. Although the observer itself does not diverge, the estimate accuracy may decay. In comparison, the consensus-based observers diverge in the presence of time delays due the integral action of the controller a system composed of quasi-average observers is more flexible and readily scalable as information about the total number of nodes N is not necessary. Table 1 presents a tabular comparison of the three control methods with their merits and demerits.

6. Case studies

We strive to achieve reactive power balance between all the DGUs in an islanded microgrid. Since the voltage restoration and reactive power sharing are coupled objectives the achievement of one deteriorates the other. We experiment with this concept and demonstrate the trade off one against the other. Figures 3a and 3b show the communication islanding scenario created to observe the effect on system performance. Table 2 gives parameters of simulation studies used in this chapter. Table 3 gives details of system loads, and Table 4 gives details of controller parameters for simulation studies.

Table 1. Comparison of observer based control strategies for time delayed communication signals.

Parameters compared	**Multiagent moving average estimation method**	**Quasi-average estimation method**	**Consensus-based methods** [38–42]
Convergence for active power	Convergence is attained	Convergence attained	Near convergence or divergence
Convergence for reactive power	Convergence attained (trade off with restoration of Voltage)	Convergence in a longer time span	Near convergence or divergence (trade off with voltage recovery)
Voltage recovery	Minimum deviations noted that decay in a very-short time period (reactive power sharing trade-off)	Minute deviations decay in a short time	Large deviations that continue partial-convergence (reactive power sharing with the trade-off)
Frequency recovery	Minimum deviations that decay in a very-short time period	Minimum deviations decline in a small period	Large deviations perceived that decline in a longer time span
Convergence time with frequency	Small	Small	Large
Voltage convergence time	Small	Small	Very large
Resilience under time-varying delays	Most	Moderate	Less
Accuracy	Most	Moderate	Moderate
Scalability	Reprogramming required for new nodes	No reprogramming required for new nodes	Some methods require reprogramming

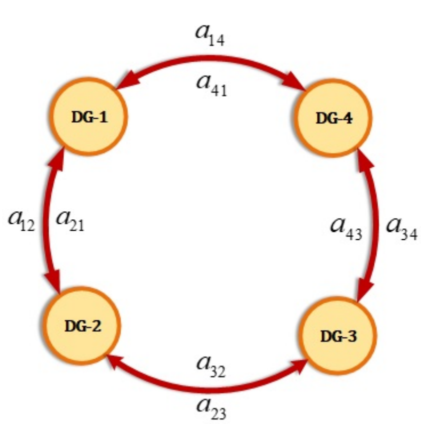

(a) Full-ring network.

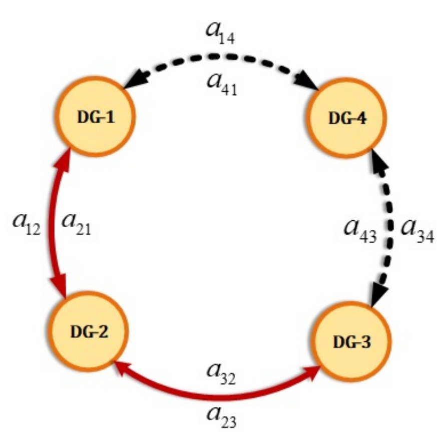

(b) Dual link latencies.

Figure 3. Node connectivity.

Table 2. Parameters for simulation studies.

Parameters	Values	Parameters	Values
L_f	$1.35mH$	m_P	4.5e-6
R_f	0.1	n_Q	1e-6
C_f	$25F$	k_{pf}	0.4
L_c	$1.35mH$	k_{if}	0.5
R_c	0.05	k_{pV}	0.5
R_{line}	0.1	k_{iV}	0.3
L_{line}	$0.5mH$	F_1	1
f_{nom}	$50Hz$	ω_c	31.41
V_{nom}	$1.1kVV_{L-L}$	S_{base}	10 kVA
		V_{base}	690 V

Table 3. System loads.

Bus no.	Bus wise connected loads	
	P(pu)	Q(pu)
1	0	0
2	0.33	0.33
3	0.33	0.33
4	0.33	0.33
5	0	0

Table 4. Controller parameters for simulation studies.

Sr.	Control parameters		
1	Power controller	Minimum	Maximum
	m_P	0.5×10^{-10}	1×10^{-5}
	n_Q	1×10^{-7}	4×10^{-3}
2	Frequency regulation		
	k_{pf}	0.4	2.5
	k_{if}	0.1	0.5
3	Voltage regulation		
	k_{pV}	0.5	3.5
	k_{iV}	0.1	0.5
3	Time delay		
	t_d	0	$2s$

6.1. Reactive power sharing

The effects of reactive power sharing on the power injection nodes are discussed in this section. The control for reactive power sharing rivals that for voltage recovery. As reactive power is efficiently exchanged, a divergence in converter node voltages is seen. Based on grid-specific conditions, a reasonable trade-off can be identified among the two objectives. The effects of reactive power sharing via the suggested controls are presented in Figure 4a.

The suggested controls' output under an injected load change is represented in Figure 4b. Figure 4c presents the identical node voltages where a deviation in node voltages is seen due to relaxed voltage restoration with more priority to reactive power sharing control. Conversely, Figure 4d shows voltage restoration with less emphasis on reactive power sharing. The reactive power sharing with consensus-based controls is shown in Figure 5a. Figure 5b shows the outcomes of reactive power sharing with suggested controls. As can be seen, the suggested method has a better reactive power sharing performance. Figure 6 presents the outcomes of power sharing under communication latencies. Figure 6a and 6b show reactive and active power sharing with suggested controls. The reactive power outcomes and the active power sharing with consensus-based controls have been seen in Figures 6c and 6d.

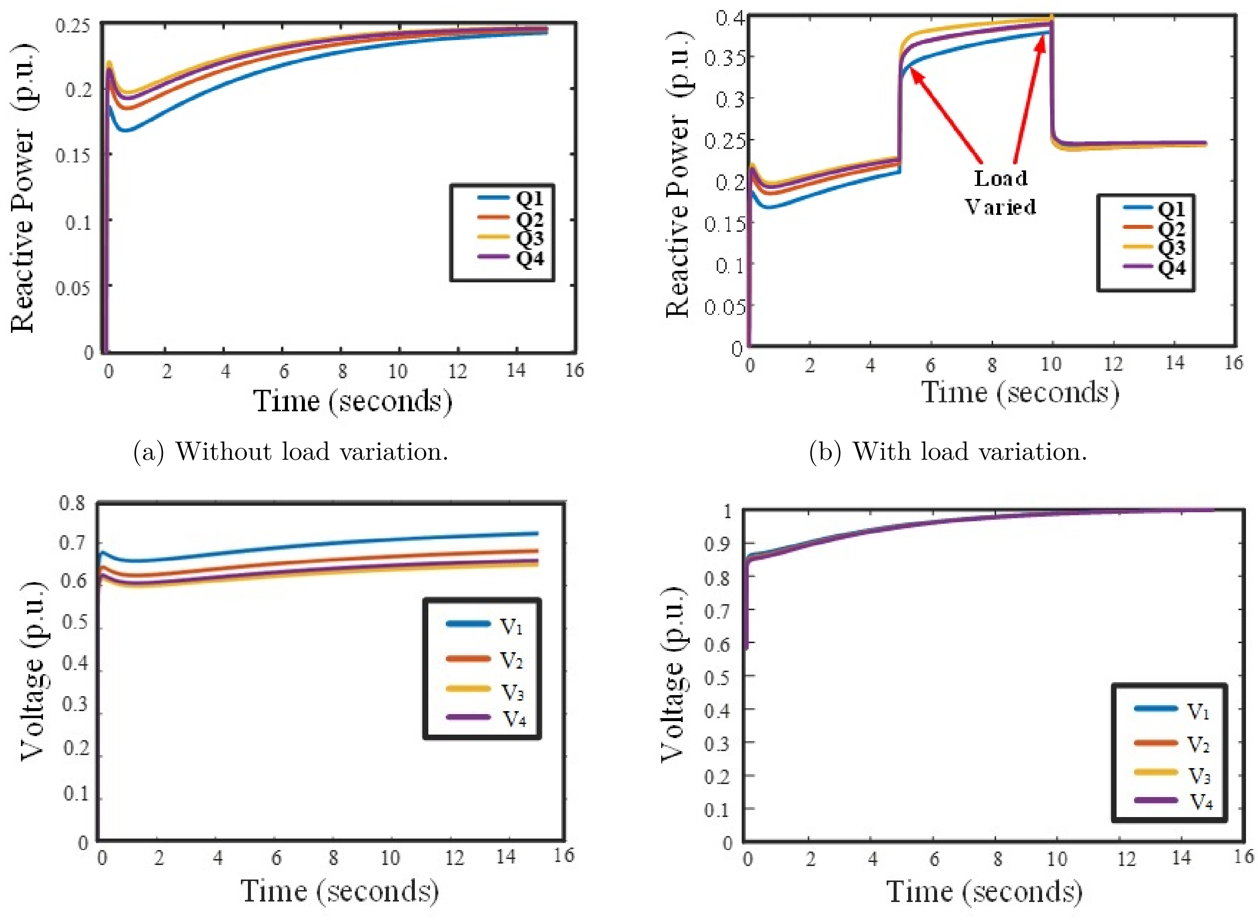

(a) Without load variation.

(b) With load variation.

(c) Voltage restoration with less priority.

(d) Voltage restoration with more priority.

Figure 4. Performance of reactive power sharing and voltage restoration under the suggested algorithm.

6.2. Variable communication time delays

The time changes added, the information signal is limited by $T_o(t)$, while the time-changing delay function is denoted as T_o as presented in Figure 7 . Figure 7a is a step delay spanning 1 s that begins at $t = 4.15$ s; at

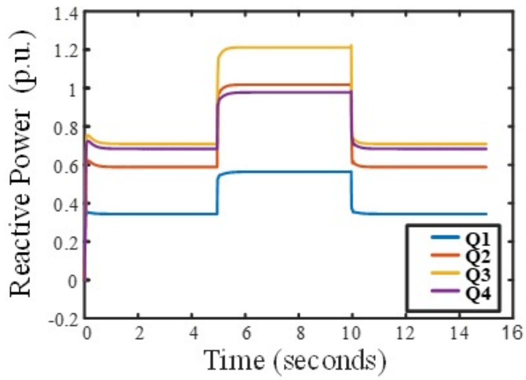

(a) Consensus-based controller.

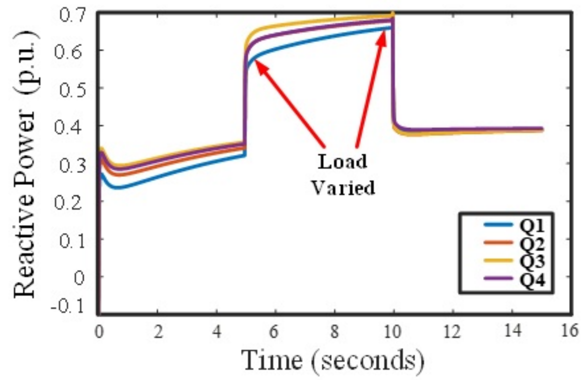

(b) Suggested controller.

Figure 5. Comparison of reactive power sharing.

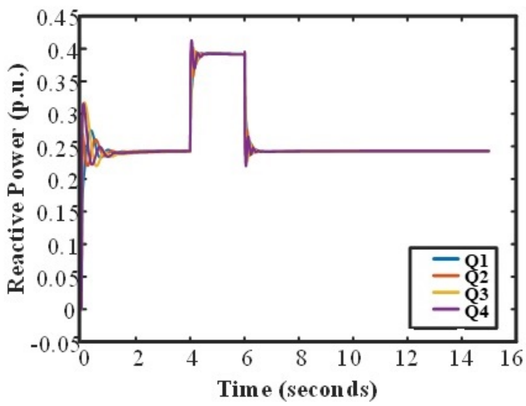

(a) Reactive power sharing with suggested system.

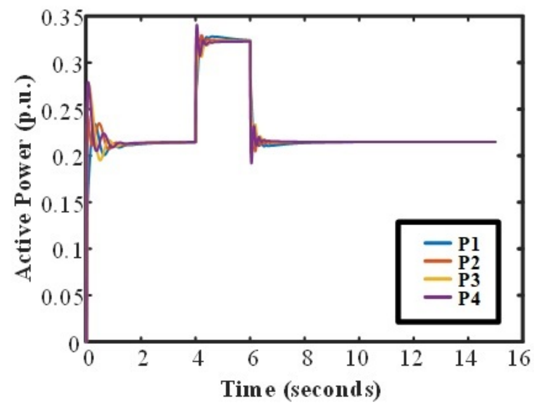

(b) Active power sharing with suggested system.

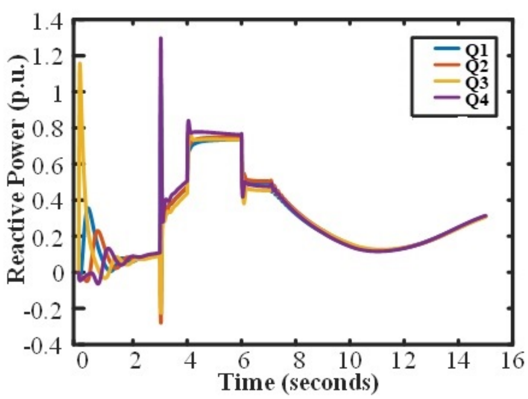

(c) Reactive power sharing with conventional control methods.

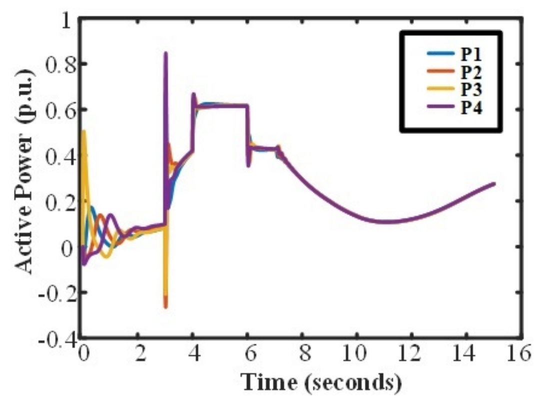

(d) Active power sharing with conventional control methods.

Figure 6. Performance of power sharing controllers under communication latencies.

$t = 5.15$ s the links are continued. In Figure 7b, a generalized delay function will represent the delay signal $y(t) = u(t - T_o(t))$, where $u(t - T_o(t))$ describes the system delayed input and $y(t)$ describes the output. There are 2 kinds of variable delays here: t_{d1} is a step delay of 1 s that starts at $t_d = 4.15$ s; at $t = 5.15$ s the links are resumed. A ramp function is denoted by t_{d2} beginning at $t = 7.5$ s and attaining the highest value at t = 10 s before abruptly dropping to zero. Load variations of $0.33pu$ are included at $t = 5$ s at busses 2, 3 and 6. At $t = 10$ s these further loads are eliminated.

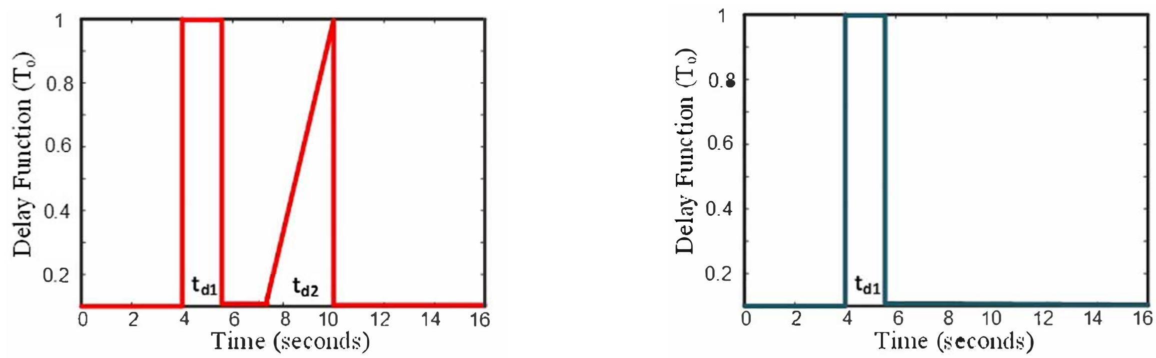

(a) Dual functions.

(b) Single function.

Figure 7. Varying time delay function.

6.3. Voltage restoration

The outcomes of voltage regulation for the suggested technique are compared in this part with consensus-based controls. Figures 8a and 8c below the suggested method reflect frequency and voltage restoration, while Figures 8b and 8d display the consensus-based design effects. Both approaches accomplish voltage recovery to optimal values. Further divergence in node voltages is observed in the consensus-based power through the first two seconds after transient start-up. The distributed power averaging approach provides voltage recovery over this initial time period without significant changes in the node's voltage. The system's converters achieve an adjustment of corrective values for active and reactive power sharing for the suggested process, therefore the power sharing, frequency and voltage of the system in a finite time frame are oriented to desired values. Nevertheless, it takes more time for the consensus-based approach to converge between device frequency and voltage. Overall, the suggested approach's outcomes present tolerance to communication delays in which specific power sharing, voltage and frequency recovery in a limited time was accomplished as voltage restorative controls compete with controls for reactive power sharing. A trade-off between the two can be established. As desired the PI controls are relaxed to less stress the voltage restoration and the reactive power sharing becomes a higher goal.

6.4. Active power sharing

A consensus observer procedure is used to verify the effectiveness of the suggested active power sharing controls. In the primary one, as shown in Figure 3, the coordination network among nodes makes a complete ring digraph. For this experiment, two subscenarios are examined. All nodes obtain input from at least two adjacent nodes. At this point, no communication delays are acknowledged. The outcomes of active power sharing with the suggested method are shown in Figure 9a, and Figure 9b provides the effects of power sharing and consensus-based monitoring of this situation. In contrast to the consensus-based approach that manifests an observable

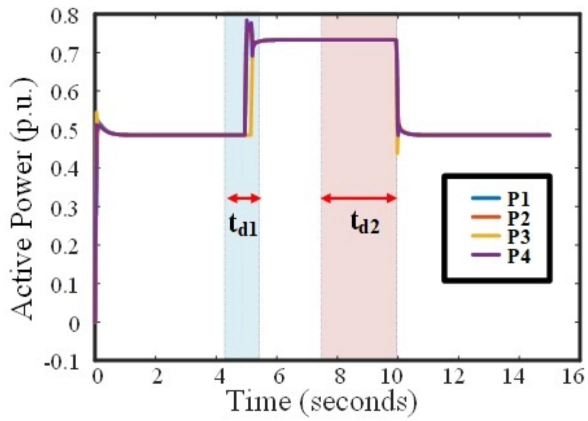

(a) Restoration of the frequency with the suggested approach.

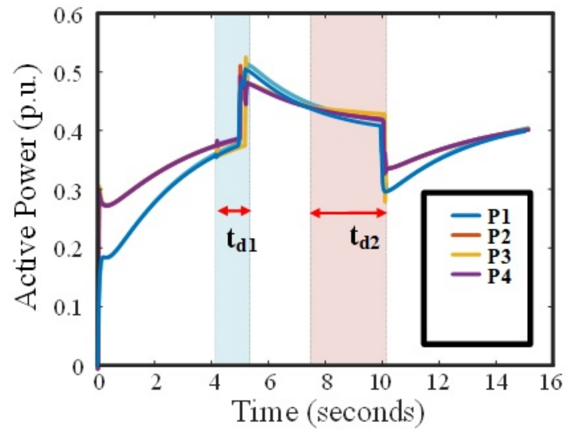

(b) Restoration of the frequency of observer consensus of neighbor nodes.

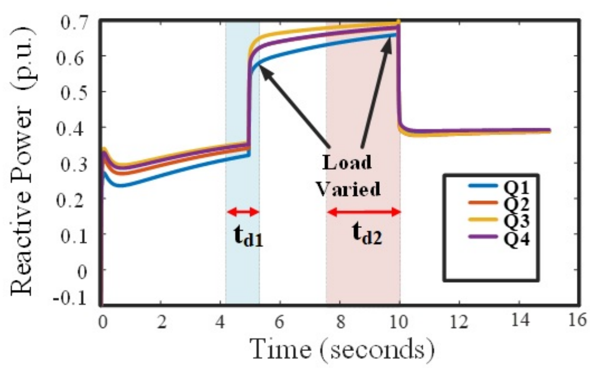

(c) Restoration of voltage with the approach suggested.

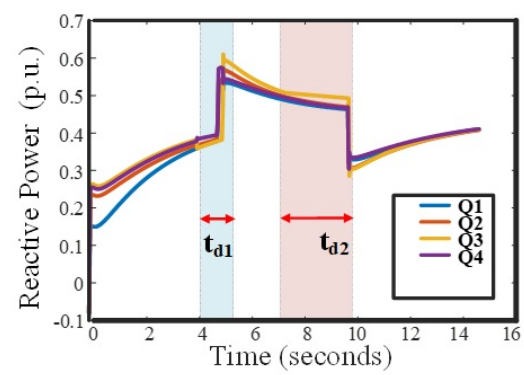

(d) Restoration of voltage with observer consensus of adjacent nodes.

Figure 8. Performance of frequency and voltage restoration controllers.

imbalance within the active power added by every node, the suggested approach delivers power sharing more efficiently. The second scenario takes into account, as presented in Figure 3b, dual-link latencies resulting to an isolated delay in the transmission of information from and to DGU-6. For this case, Figure 9c to Figure 9d compares the effects of reactive power sharing according to the suggested average based approach and consensus observer-based control. In the consensus-based approach, a divergence in added powers can be observed, and the trend to convergence is slow. Whereas, within a finite time, the suggested approach achieves good reactive power sharing and the convergence rate is faster.

6.5. Frequency restoration

For this case, Figure 9c to Figure 9d compares the effects of reactive power sharing according to the suggested average based approach and consensus observer-based control. In the consensus-based approach, a divergence in added powers can be seen, and the trend to convergence is slow. Whereas, within a finite time, the suggested approach achieves good reactive power sharing and the convergence rate is faster.

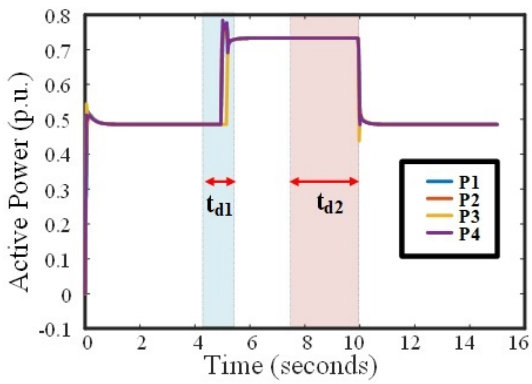

(a) Active power sharing with suggested method.

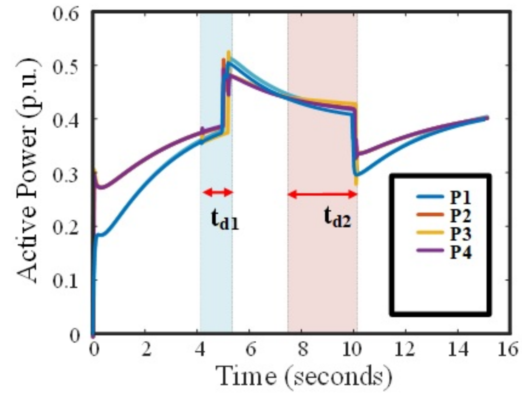

(b) Active power sharing with consensus-based method.

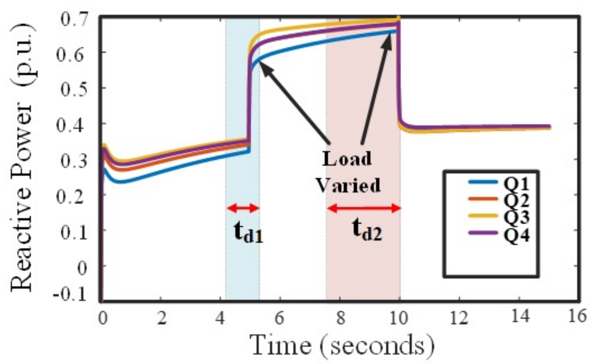

(c) Reactive power sharing with suggested method.

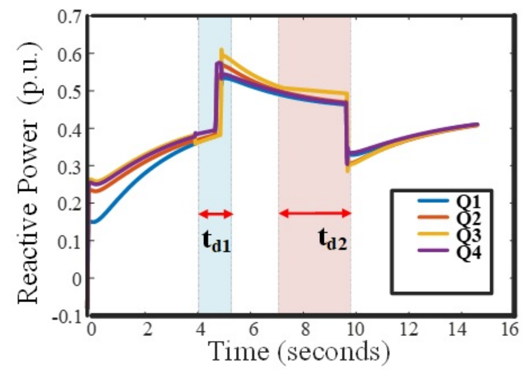

(d) Reactive power sharing with a method based on consensus.

Figure 9. Comparison of active and reactive power sharing using suggested and consensus-based power controllers.

7. Experimental results

This part describes the experimental results collected from the lab-scale MG test bench developed during this work. The set-up is composed of two power inverters each rated at 60 KVA. However, for experimental purposes and keeping in view equipment protection, these were operated only at a maximum level of 105 V (rms) and 7 A (rms). Table 5 gives the details of controller gains used in this experiment.

7.1. Active power distribution results

The active power sharing is computed based on instantaneous voltage and current readings obtained at inverter terminals. As demonstrated in earlier section, low pass filters are used to remove higher order harmonics. Figure 8 shows the results of active power distribution between DGU nodes. Each inverter in the system is initially injecting around 100 Watt the system loads. The load is increased at t = 5 s from 300 Watt (100 Watt/DGU) to nearly 1350 Watt (450 Watt/DGU) using R-L loads. It can be seen from Figure 10 that the three DGUs share this load equally due to the effect of the suggested control scheme. At t = 10 s the collective loads are reduced to the previous level at 300 Watt. These instantaneous power curves can be observed in Figure 10 where the power sharing controls are operating effectively.

Table 5. Controller parameters for experiment.

Parameters		Symbol	Values
Nominal frequency		f*	50 Hz
Nominal voltage		V*	100 V (rms)
Switching frequency		fs	16 kHz
DC source voltage		VDC	200 V
DC source current (Max)		IDC	20 A
Zero level controllers	Voltage loop controller	KpV1	23
		KiV1	55
	Current loop controller	KpC1	42
		KiC1	110
Primary controllers	Active power controller	mPi	0.00035 Rad /Watt
	Reactive Power controller	nQi	0.00001 Volt /VA
Secondary controllers	Voltage restorative controller	KpVr	2.5
		KiVr	0.5
	Frequency restorative controller	Kpfr	3.5
		Kifr	0.8
Communication delay		td	10 ms (min)-2 s(max)

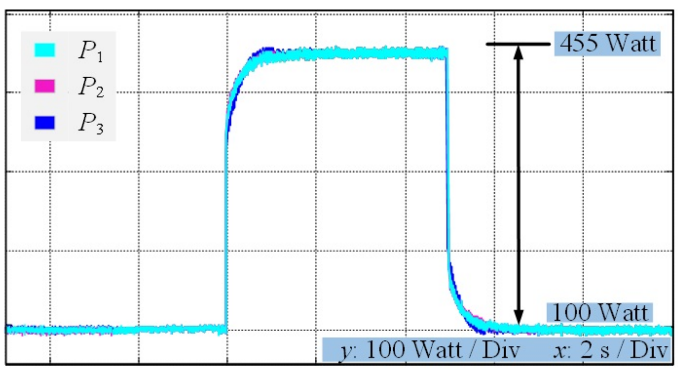

Figure 10. Active power distribution between DGUs.

7.2. Reactive power distribution results

The reactive power sharing is computed based on instantaneous voltage and current readings using Ethernet modules installed on-board each converter unit. The power calculator is used for measuring reactive power values in the algorithm and the low pass filters are used to eliminate harmonics of higher order. The reactive power sharing results utilizing the suggested controllers are shown in Figure 11a. The system loads are drawing a collective reactive load of around 120 VAR (nominally 40 VAR/DGU). This load is being shared by the three DGU units nearly equally due to the effect of the suggested system. At t = 5 s, the reactive load on the system is increased to 420 VAR (nominally 138 VAR/DGU). The increase in the reactive power demand is equally shared between all three DGUs and the reactive power sharing remains stable. The suggested controllers regulate the reactive power sharing and keep the power contributed by each DGU nearly equal. At t = 10 s, the additional reactive load is removed and the power returns to previous values. Figure 11b shows the load reactive power increase transient. Figure 12 shows the regulation of reactive power between DGUs using conventional droop-based control. As can be seen, the reactive power is not effectively shared between DGUs using conventional droop-based method.

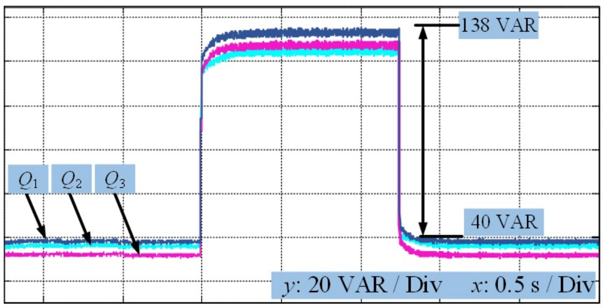

(a) Reactive power with load variations.

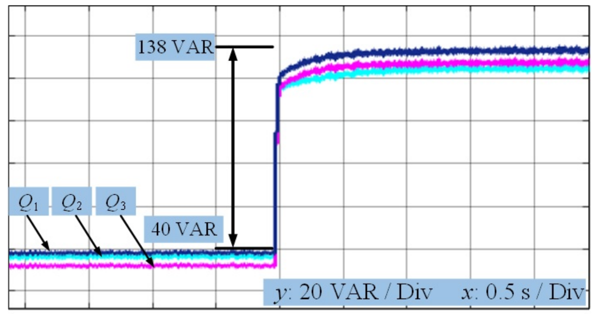

(b) Reactive power with load variations.

Figure 11. Reactive power sharing.

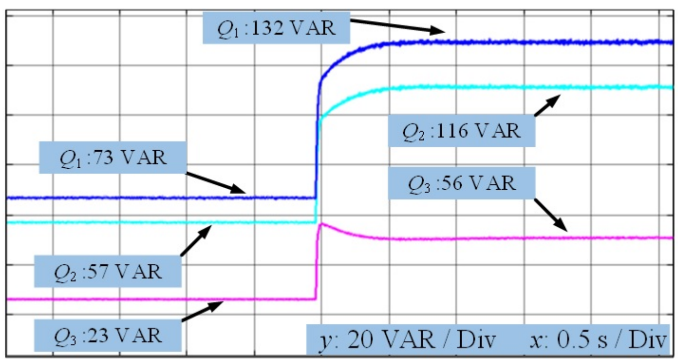

Figure 12. Reactive power sharing with conventional control methods.

7.3. Frequency regulation results

The frequency at inverter terminals is measured using voltage sensors connected to the Ethernet modules onboard each DGU unit. The platform developed in LabView receives these values and the frequency is computed using PLL calculation. Figure 13a shows the performance of frequency restoration controllers in a consensus-based control scheme with communication links having latencies. Figure 13b shows the frequency restoration using the suggested strategy. It can be observed that a there is a visible deterioration in the frequency restoration performance during communication latencies and the system frequency cannot be properly restored, whereas, with the suggested control scheme the system frequency remains at the nominal value and returns to nominal values following load change transients.

7.4. Voltage regulation results

The voltage at inverter terminals is measured using voltage sensors. LabView reads these values periodically. Figure 14 shows the performance of secondary voltage restoration controllers under load variations. As can be seen, the voltage restoration controllers regulate the system voltage to the nominal level.

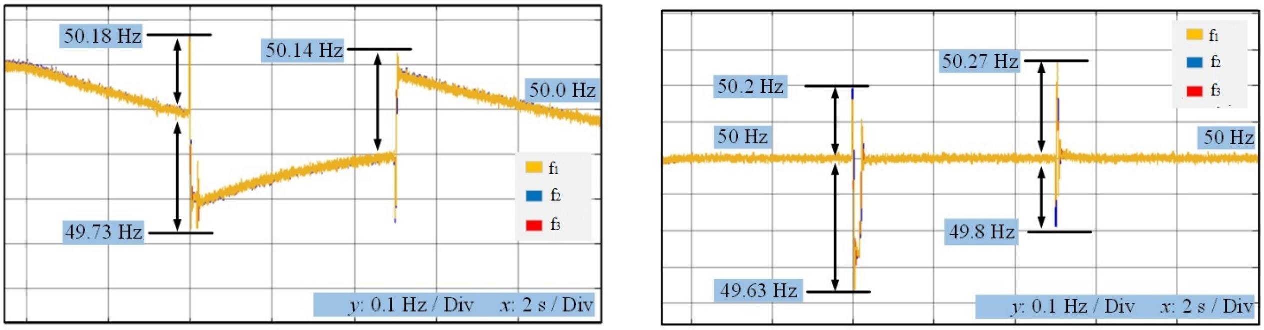

(a) Consensus-based control. (b) Suggested control method.

Figure 13. Frequency restoration.

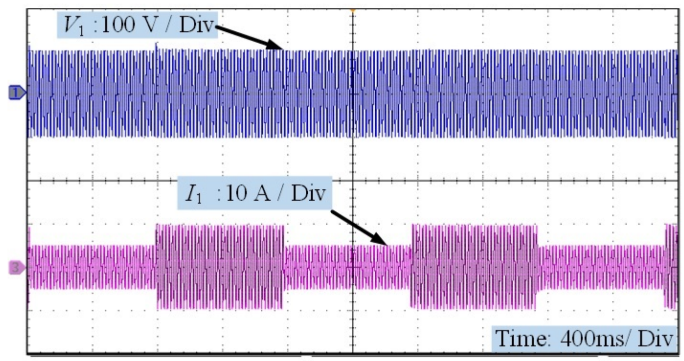

Figure 14. Voltage and current of phase-A with load variations.

8. Discussion

A coupling exits between reactive power sharing and voltage recovery objectives. The nature of the linkage between these two is such that only one may be completely achieved at one time. If the voltage is completely and accurately restored the reactive powers will not be equivalently shared. On the other hand, if the reactive powers are effectively shared between the nodes, voltage restoration cannot be simultaneously achieved. Therefore, a compromise between the two objectives is worked out such that both the objectives may be achieved to some extent. On the other hand, active power may be accurately shared using droop controllers and frequency restoration may also be achieved on a slower time scale. The reactive power sharing controller operates over a narrower margin than the active power sharing and is prone to greater instability and may fail to converge system states in the presence of greater disturbances.

9. Conclusion

The distribution of reactive power between DGU nodes is important to maintain in the absence of flexible transmission devices at the low and medium voltage network level. It is challenging to distribute reactive power between MG nodes when the voltage is also being restored in the secondary layer. The traditionally employed Q-V droop does not satisfactorily achieve this control objective. The power sharing problem is a challenging one for isolated community networks such as microgrids and microgrid clusters that have DGUs situated in proximity and are often trading energy with their neighbors. This paper proposes a distributed cooperative control scheme that discusses reactive power balancing in inverter-based island microgrids for effective reactive power sharing and simultaneous voltage recovery. Furthermore, the control scheme is made resilient to communication link delays and latencies. This paper presents a test MG structure and simulations of case studies are carried out to determine the efficacy of the suggested methodology. The suggested control scheme is compared against conventional power sharing and restorative control for microgrids. A comparative discussion among conventional consensus-based controls, the quasi-average technique and the multiagent moving average method is made for completeness to this thesis. This comparison reveals that while both the suggested methods are superior to the conventional consensus-based control schemes in practice so far, the multiagent moving average method shows better results than the quasi-average method in terms of accuracy and faster convergence. To further establish the efficacy of the suggested control methods, experimental studies are conducted on the limited scale MG set up developed in our lab. The experimental results further reflect the suggested control method's relative superiority over other conventional consensus-based control methods used for MG control.

References

[1] Han Y, Zhang K, Li H, Coelho EAA, Guerrero JM. Mas-based distributed coordinated control and optimization in microgrid and microgrid clusters: A comprehensive overview. IEEE Transactions on Power Electronics 2017; 33 (8): 6488–6508. doi: 10.1109/TPEL.2017.2761438

[2] Guerrero JM , Chandorkar M , Lee TL, Loh PC. Advanced control architectures for intelligent microgridspart i: Decentralized and hierarchical control, IEEE Transactions Industrial Electronics 2013; 60 (4):1254–1262 doi: 10.1109/TIE.2012.2194969

[3] de Souza WF, Severo-Mendes MA, Lopes LA. Power sharing control strategies for a three-phase microgrid in different operating condition with droop control and damping factor investigation. IET Renewable Power Generation 2015; 9 (7): 831–839. doi: 10.1049/iet-rpg.2014.0250

[4] Han H, Hou X, Yang J, Wu J, Su M et al. Review of power sharing control strategies for islanding operation of ac microgrids. IEEE Transactions on Smart Grid 2015; 7 (1): 200–215. doi: 10.1109/TSG.2015.2434849

[5] Palizban O, Kauhaniemi K. Hierarchical control structure in microgrids with distributed generation: Island and grid-connected mode. Renewable and Sustainable Energy Reviews 2015; 44: 797–813. doi: 10.1016/j.rser.2015.01.008

[6] Zhu Y, Zhuo F, Wang F, Liu B, Gou R, et al. A virtual impedance optimization method for reactive power sharing in networked microgrid. IEEE Transactions on Power Electronics 2015; 31 (4): 2890–2904. doi: 10.1109/TPEL.2015.2450360

[7] Mahmud M, Hossain M, Pota H, Oo A. Robust nonlinear distributed controller design for active and reactive power sharing in islanded microgrids. IEEE Transactions on Energy Conversion 2014; 29 (4): 893–903. doi: 10.1109/TEC.2014.2362763

[8] Wang J, Chang NCP, Feng X, Monti A. Design of a generalized control algorithm for parallel inverters for smooth microgrid transition operation. IEEE Transactions on Industrial Electronics 2015; 62 (8): 4900–4914. doi: 10.1109/TIE.2015.2404317

[9] Green TC, Prodanovi CM. Control of inverter-based micro-grids. Electric power systems research 2007; 77 (9): 1204–1213. doi: 10.1016/J.EPSR.2006.08.017

[10] Schiffer J, Seel T, Raisch J, Sezi T. Voltage stability and reactive power sharing in inverter-based microgrids with consensus-based distributed voltage control. IEEE Transactions on Control Systems Technology 2015; 24 (1): 96–109. doi:10.1109/TCST.2015.2420622

[11] Nelson M, Jordan PE. Automatic reconfiguration of a ship's power system using graph theory principles. IEEE Transactions on industry applications 2014; 51(3): 2651–2656. doi: 10.1109/TIA.2014.2365622

[12] Lee CT, Chu CC, Cheng PT. A new droop control method for the autonomous operation of distributed energy resource interface converters. IEEE Transactions on Power Electronics 2012; 28 (4): 1980–1993. doi: 10.1109/TPEL.2012.2205944

[13] He J, Li YW. An enhanced microgrid load demand sharing strategy. IEEE Transactions on Power Electronics 2012; 27 (9): 3984–3995. doi: 10.1109/TPEL.2012.2190099

[14] Simpson-Porco JW, Shafiee Q, Dörfler F, Vasquez JC, Guerrero JM et al. Secondary frequency and voltage control of islanded microgrids via distributed averaging. IEEE Transactions on Industrial Electronics 2015; 62 (11): 7025–7038. doi: 10.1109/TIE.2015.2436879

[15] Zeng Z, Yang H, Zhao R, Cheng C. Topologies, and control strategies of multi-functional grid-connected inverters for power quality enhancement: A comprehensive review. Renewable and Sustainable Energy Reviews 2013; 24: 223–270. doi: 10.1016/j.rser.2013.03.033

[16] Hamzeh M, Mokhtari H, Karimi H. A decentralized self-adjusting control strategy for reactive power management in an islanded multi-bus mv microgrid. Canadian Journal of Electrical and Computer Engineering 2013; 36 (1): 18–25. doi: 10.1109/CJECE.2013.6544468

[17] Zhu Y, Zhuo F, Shi H. Accurate power sharing strategy for complex microgrid based on droop control method. In 2013 IEEE ECCE Asia Downunder. IEEE 2013; 344–350. doi: 10.1109/ECCE-Asia.2013.6579119

[18] Wang Y, Chen Z, Wang X, Tian Y, Tan Y et al. An estimator-based distributed voltage-predictive control strategy for ac islanded microgrids. IEEE Transactions on Power Electronics 2014; 30 (7): 3934–3951. doi: 10.1109/TPEL.2014.2345696

[19] Savaghebi M, Jalilian A, Vasquez JC, Guerrero JM. Autonomous voltage unbalance compensation in an islanded droop-controlled microgrid. IEEE Transactions on Industrial Electronics 2012; 60 (4): 1390–1402. doi: 10.1109/TIE.2012.2185914

[20] He J, Li YW, Blaabjerg F. An enhanced islanding microgrid reactive power, imbalance power, and harmonic power sharing scheme. IEEE Transactions on Power Electronics 2014; 30 (6): 3389–3401. doi: 10.1109/TPEL.2014.2332998

[21] Milczarek A, Malinowski M, Guerrero JM. Reactive power management in islanded microgrid proportional power sharing in hierarchical droop control. IEEE Transactions on Smart Grid 2015; 6 (4): 1631–1638. doi: 10.1109/TSG.2015.2396639

[22] Kekatos V, Wang G, Conejo AJ, Giannakis GB. Stochastic reactive power management in microgrids with renewables. IEEE Transactions on Power Systems 2014; 30 (6): 3386–3395. doi: 10.1109/TPWRS.2014.2369452

[23] Li Q, Chen F, Chen M, Guerrero JM, Abbott D. Agent-based decentralized control method for islanded microgrids. IEEE Transactions on Smart Grid 2015; 7 (2): 637–649. doi:10.1109/TSG.2015.2422732

[24] Liu S, Wang X, Liu PX. Impact of communication delays on secondary frequency control in an islanded microgrid. IEEE Transactions on Industrial Electronics 2014; 62 (4): 2021–2031. doi: 10.1109/TIE.2014.2367456

[25] Ahumada C, Cárdenas R, Saez D, Guerrero JM. Secondary control strategies for frequency restoration in islanded microgrids with consideration of communication delays. IEEE Transactions on Smart Grid 2016; 7(3): 1430–1441. doi: 10.1109/TSG.2015.2461190

[26] Nasirian V, Shafiee Q, Guerrero JM, Lewis FL, Davoudi A. Droop-free distributed control for ac microgrids. IEEE Transactions on Power Electronics 2015; 31 (2): 1600–1617. doi: 10.1007/978-3-319-50808-5_6

[27] Mohamed YARI, Radwan AA. Hierarchical control system for robust microgrid operation and seamless mode transfer in active distribution systems. IEEE Transactions on Smart Grid 2011; 2 (2): 352–362. doi: 10.1109/TSG.2011.2136362

[28] Kahrobaeian A, Mohamed YARI. Networked-based hybrid distributed power sharing and control for islanded microgrid systems. IEEE Transactions on Power Electronics 2014; 30 (2): 603–617. doi: 10.1109/TPEL.2014.2312425

[29] Nutkani IU, Loh PC, Wang P, Blaabjerg F. Autonomous droop scheme with reduced generation cost. IEEE Transactions on Industrial Electronics 2014; 61 (12): 6803–6811. doi: 10.1109/TIE.2014.2314056

[30] Das S, Nutkani IU, Teixeira C. Decentralised master slave control for series cascaded islanded ac microgrid. IEEE Transactions on Industrial Electronics 2021. doi: 10.1109/TIE.2021.3094414

[31] Lu J, Zhao M, Golestan S, Dragicevic T, Pan X et al. Distributed event-triggered control for reactive, unbalanced, and harmonic power sharing in islanded ac microgrids. IEEE Transactions on Industrial Electronics 2021. doi: 10.1109/TIE.2021.3057018

[32] Zhang Y, Shotorbani AM, Wang L, Mohammadi-Ivatloo B. Distributed secondary control of a microgrid with a generalized pi finite-time controller. IEEE Open Access Journal of Power and Energy 2021; 8: 57–67 doi: 10.1109/oajpe.2021.3056507

[33] Li X, Chen C, Xu Q, Wen C. Resilience for communication faults in reactive power sharing of microgrids. IEEE Transactions on Smart Grid 2021 doi: 10.1109/TSG.2021.3060917

[34] Nguyen DH, Khazaei J. Unified distributed control of battery storage with various primary control in power systems. IEEE Transactions on Sustainable Energy 2021. doi: 10.1109/tste.2021.3091976

[35] Baharizadeh M, Golsorkhi MS, Shahparasti M, Savaghebi M. A two-layer control scheme based on p-v droop characteristic for accurate power sharing and voltage regulation in dc microgrids. IEEE Transactions on Smart Grid 2021. doi: 10.1109/TSG.2021.3060074

[36] Shenoi BA. Introduction to digital signal: Processing and filter design, 1st ed. Hoboken, New Jersey: John Wiley & Sons, INC., 2006.

[37] Bidram A, Nasirian V, Davoudi A, Lewis FL. Cooperative synchronization in distributed microgrid control, 1st ed. Springer International Publishing, 2017.

[38] Bidram A, Davoudi A, Lewis FL, Guerrero JM. Distributed cooperative secondary control of microgrids using feedback linearization. IEEE Transactions on Power Systems 2013; 28 (3): 3462–3470. doi: 10.1109/TPWRS.2013.2247071

[39] Zuo S, Davoudi A, Song Y, Lewis FL. Distributed finite-time voltage and frequency restoration in islanded ac microgrids. IEEE Transactions on Industrial Electronics 2016; 63 (10): 5988–5997. doi: 10.1109/TIE.2016.2577542

[40] Guo F, Wen C, Mao J, Song YD. Distributed secondary voltage and frequency restoration control of droop-controlled inverter-based microgrids. IEEE Transactions on industrial Electronics 2014; 62 (7): 4355–4364. doi: 10.1109/TIE.2014.2379211

[41] Wang Y, Wang X, Chen Z, Blaabjerg F. Distributed optimal control of reactive power and voltage in islanded microgrids. In 2016 IEEE Applied Power Electronics Conference and Exposition (APEC). IEEE, 20163; 431–3438. doi: 10.1109/TIA.2016.2615033

[42] Schiffer J, Seel T, Raisch J, Sezi T. Voltage stability and reactive power sharing in inverter-based microgrids with consensus-based distributed voltage control. IEEE Transactions on Control Systems Technology 2015; 24 (1): 96–109. doi: 10.1109/TCST.2015.2420622